Electromechanical properties of narrow superconducting cables comprised of exfoliated YBCO filaments

Vyacheslav Solovyov, Saad Rabbani, Monan Ma, Zachary Mendleson, Zhen Wang, Analolii Polyanskii and Paul Farrell

***Abstract*— Development of multifilament YBCO cables is an important step towards manufacture of practical superconducting magnets based on second generation high temperature superconductor technology. Currently, magnets manufactured from wide 2G tapes suffer from high magnetization loss, and poor reliability. The presence of an insulation substrate insulates YBCO layers from each other, which allows only for lateral (along the tape face) current sharing. Here we show that exfoliated multilayer cable with electrically coupled, narrow (< 1 mm wide) filaments allow for normal (across the tape) current sharing within the cable. This development can potentially enable fast ramping stable high-field magnets for applications in fusion, energy storage and transportation.**

***Index Terms*— High-temperature superconductors, multifilamentary superconductors, laser processing**

I. Introduction

SECOND generation conductors (2G) are the enabling technology for the future high-field cryogen-free magnets operating at 20-30 K. At ≈ 30 K a compact and inexpensive single stage cryocooler can deliver enough power to cool down a medium-size magnet within several hours. However, architecture of the traditional 2G tapes makes them a less than an ideal fit for many applications. Wide and thin 2G conductors have high magnetic moment and high hysteretic (AC) loss. High AC loss prevents wider penetration of 2G conductors into power equipment markets, where operation in ≈ 60 Hz alternating magnetic field is often desired. High field error of 2G magnets limits limit their application as NMR inserts [1, 2] or accelerator dipoles.

The work at Brookhaven Technology Group was supported by the Department of Energy, Office of High Energy Physics under SBIR Phase I award DE-SC0017797. M. M. and Z. M. were supported in part by Office of Strategic Partnership for Industrial Resurgence at Stony Brook University.

(Corresponding *author: Vyacheslav Solovyov)*

V. F. Solovyov is with Brookhaven Technology Group, 1000 Innovation Road, Stony Brook, NY 11794, (slowa@brookhaventech.com).

S. Rabbani is with Brookhaven Technology Group, 1000 Innovation Road, Stony Brook, NY 11794, (saad.rabbani@brookhaventech.com).

P. Farrell is with Brookhaven Technology Group, 1000 Innovation Road, Stony Brook, NY 11794, (pfarrell@brookhaventech.com).

Monan Ma and Zachary Mendleson and Zhen Wang are with Stony Brook University, Stony Brook, NY 11794

Analolii Polyanskii is with National High Magnetic Field Laboratory, 2031 E. Paul Dirac Dr. Tallahassee , FL 32310 (polyanskii@asc.magnet.fsu.edu)

Digital Object Identifier.

It is well known that narrow transposed superconducting filaments are the essential ingredients of a low-loss superconducting cable and, consequently of a magnet with low field error [3]. Several approaches to patterning of the superconducting YBCO layers into narrow stripes have been explored by various groups [4-6]. A reduction of magnetization loss in coil manufactured from patterned 2G tape is well documented [7, 8]. However, the patterning approach yields a cable with electrically isolated un-transposed filaments and negligible current sharing.

Reliable current sharing between filaments is critical for 2G cables with ≈ 1 mm filament width because manufacturing epitaxial YBCO layer free of current-limiting defects is difficult. In a narrow filament the probability of a defect blocking superconducting current increases inversely proportional to the filament width. For example, a typical continuous coupon of 10 mm wide 2G tape manufactured today is ≈ 100 m long. If this tape coupon were patterned or sliced into 1 mm wide filaments, the resulting continuous length of a 1 mm filament would be significantly shorter, on the order of 10 m. In a patterned tape lateral current sharing can be realized by shortening the filaments with a normal metal, however the coupling losses of such a cable would increase to the level hysteretic losses of the original wide tape. Several multifilament cabling approaches that are being explored, such as twisted stack [9, 10], spiral-wound cable [11] and Roebel cable [12] involve using the traditional 2G tapes as filaments. In these cable designs the current sharing is not addressed because the insulating substrate impedes current transfer between filaments.

In this contribution we report properties of 1.0 mm wide cables comprised of exfoliated YBCO filaments [13]. The exfoliated filaments are manufactured by separation YBCO layer from the oxide substrate. The process eliminates the current-blocking oxide buffer layer thus allowing for normal (across the filament face) current sharing. This filaments are stacked vertically thus the effective width of the cable is equal to the filament width. Therefore the current sharing can be achieved without penalty of higher hysteretic or coupling losses. We show that modern laser cutting technologies are capable of rapid slicing of exfoliated tapes into < 1 mm wide filaments with minimal edge damage.

II. Experiment

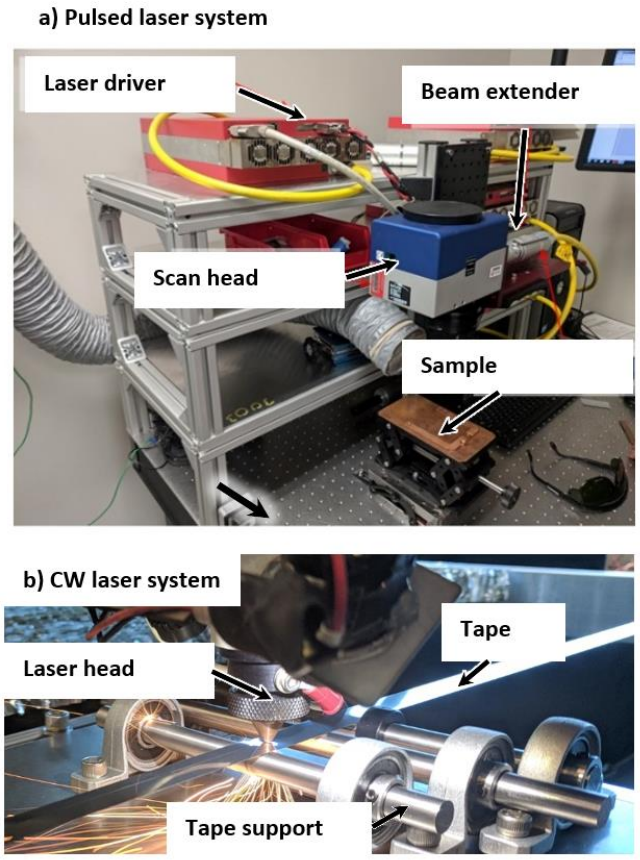

Fig. 1. (a) Pulsed fiber laser slicing setup. (b) Reel-to-reel CW CO2 laser slicing setup, based on Kern laser HSE 200 W laser cutter.

Commercially available 10 mm wide 2G tapes were exfoliated following a procedure described in [13], and sliced into 2-1 mm wide filaments using a variety of laser techniques: a continuous wave (CW) laser and pulsed lasers with 80, 2 and 10 ps pulse width.

Fig. 1a shows the experimental setup used in the filamentization of short, 10 cm long, test coupons with a pulsed laser. Briefly, a pulsed diode fiber laser system delivered a 80 ns pulsed beam of 1.06 μm light to a collimator with 7.5 mm aperture and then delivered the samples surface by a RayLase scan-head equipped with a 100 mm F-theta lens, Eksam Optics FTH100-1064. The scan-head rastered the laser beam to produce 2 mm and 1 mm wide, 10 cm long, strips. The F-theta lens ensured that the laser beam remained in focal position as the beam is rastered over a flat area. The beam was moved at fixed speed of 300 mm/s. A similar arrangement was employed for slicing with 2 ns and 10 pulses, however the cutting speed was lower, 2 mm/s due to a lower power, ≈ 2 W, of short-pulse lasers.

Fig. 1b shows reel-to-reel CW slicing system based Kern Lasers HSE model CO_2 laser. The laser beam was delivered through a gas nozzle, which also supplied a constant stream of oxygen into the cut area. The supplied laser processing table was equipped with a custom tape motion and positioning system. Up to 10 meter long, 1 mm wide filament coupons were sliced using the reel-to-reel CO2 laser system shown in Fig. 1 b. After slicing, the filaments were coated with Sn62Pb36Ag02 solder by a reel-to-reel dip coating process. Prior to the solder coating, the filament entered a flux bath filled with 2331-ZX flux (Kester Illinois Tool Works Company). The solder coating was performed at 1 cm/s tape speed with a solder bath temperature of 240ºC. The coated filaments were arranged in a stacked array and wrapped with AWG 40 Nichrome wire. In this experiment, the cable was comprised of eight and four, 1.0 mm wide YBCO filaments sandwiched between two, 0.9 mm wide, 0.16 mm thick stainless steel 304 ribbons. The total cable thickness was thus approximately 1.0 mm and 0.6 mm for eight and four filament cable correspondingly. Mini test coils were made by winding a cable around an 80 mm diameter G10 tube under 10 N tension.

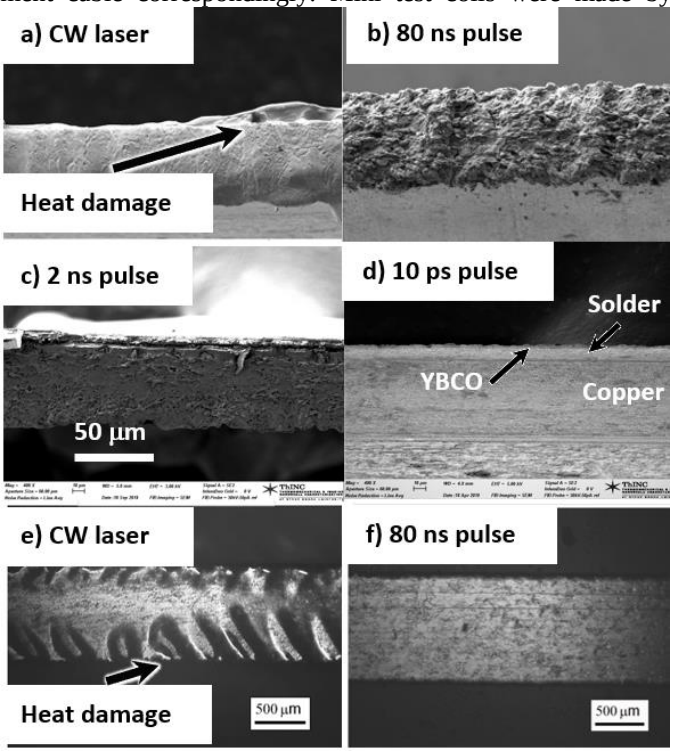

Fig. 2. (a-d) Scanning electron microscopy cross-sections of exfoliated filament cut with various laser types. (a) continuous wave (CW) CO2 laser. (b) 80 ns 1.056 mm pulsed fiber laser. (c) 2 ns pulsed. (d) 10 ps nm pulsed. (e-f) Optical micrographs of 1 mm wide filaments sliced using: (e) CW CO2 laser. (f) Plane view of 1 mm filament sliced using 80 ns pulsed laser. Note reduction of the heat damage area, well visible as striation features in panel (e). Panel (d) also shows architecture of the exfoliated filament.

The coil assembly was placed in a furnace for the re-flow step. During the reflow, the coil was heated to 185ºC. The solder coating of the YBCO filaments partially melted, thus fusing the filaments into an electrically and mechanically coupled solid. After the re-flow step the coils were tested at 77 K.

III. Results and Discussion

Fig. 2 is a side-by-side comparison of scanning electron microscopy (SEM) edge view micrographs of filaments sliced using CW CO2 laser (a), 80 ns pulse laser (b), 2 ns and 100 ps in panels (c) and (d). Edge of the sample cut by CO_2 CW laser show clear signs of material melting, with characteristic

droplets of melted material, or slug, well visible on the bottom of the cut. The heat damage to the YBCO layer can be seen as buckling of the YBCO layer in Fig. 2e. In contrast, the edge of the samples cut by the pulsed lasers is a conglomerate of small droplets of molten metal. The amount of droplets and the cut becomes cleaner as the pulse with is shortened to 2 ns and 10 ps. This edge appearance in Fig. 2d-c is consistent ablation, i.e. material removal by evaporation without melting. Edge view of 10 ps cut, Fig. 2d is typical for the photo-ablation regime when a material is removed by direct breaking of chemical bonds by radiation without the evaporation phase. Fig. 3a is a summary of I_c vs. filament width dependences for filaments cut with a pulsed 80 ns laser and CO_2 CW fiber lasers. Properties of filaments cut with 2 ns and 10 ps lasers were essentially identical to filaments processed with the 80 ns laser. The dashed rectangle shows the level of the original I_c for 10 mm wide tape.

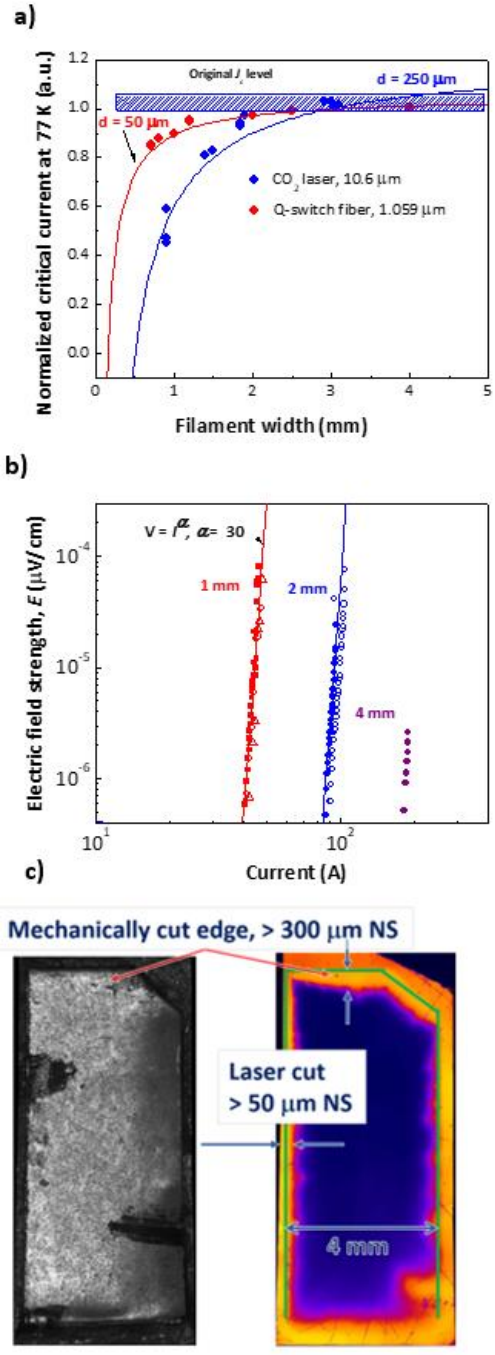

Fig. 3. (a) Dependence of the critical current density on the filament width. The solid lines represent best fits using Eq. 1. (b) *I-V* curves of 1, 2 and 4 mm filaments sliced with the pulsed 80 ns laser. The solid lines are best fits of the data using $V \sim I^{\alpha}$ function, where $\alpha = 30$. (c) Magneto-optic images of a filament sliced with 80 ns pulse laser, comparing edge damage of the laser slicing and mechanical cut. The mechanical cut leaves approximately 300 μm wide non-superconducting area, compared with 50 μm wide damage caused by the laser slicing. Residual field image, 10 K.

The solid lines are best fit approximations by the following function which described dependence of I_c of a filament of width w, assuming the that edge damage zones of width d are non-superconducting:

$$I_c(w) = I_c(1 - {}^{2d}/_{w}) \quad (1)$$

Here the only fitting parameter is d. Eq. 1 predicts that when $w = 2d$, that is the edge damage zones would overlap and the effective critical current would be zero. The approximations show that for filaments sliced with the pulsed 80 ns laser, $d = 45 \pm 10$ μm. However, for the CO_2 CW lasers, $d = 200 \pm 20$ μm. This is consistent with the analysis of magneto-optical image of a laser sliced filament shown in Fig. 3c. Fig. 3c also compares the damage zone of the laser with that one of a mechanical cut. The mechanical cut damages ≈ 300 μm wide band of superconductor compared to only 50 μm wide damage zone when 80 ns laser is used.

Shorter pulses are obviously beneficial in preventing the heat damage of the filament The photoablation regime, achieved with > 100 ps pulses appears to be the most desirable in terms of thermal damage and the cut accuracy. However the available sub-ns laser processing systems are still expensive. In order to estimate the maximum acceptable laser pulse duration that still does not overheat the filament edge we calculate the thermal equilibration time τ of the filament. The thermal equilibration time, defined as the time it takes for the thermal wave to propagate the foil thickness through the thermal diffusion process. If a sample pulse is shorter than the thermal equilibration time and the pulse energy is sufficient to ablate the material, most of the thermal energy will be carried away by the material vapor rather than by the convection cooling by the assist gas [14]. The copper stabilizer is the dominant contribution to the thermal equilibration time:

$$\tau = \frac{C_v \rho t^2}{4K} \quad (2)$$

Where C_v is specific heat, ρ is the filament material density, t is the filament thickness and K is the thermal conductivity. For 75 μm thick copper foil $\tau = 12$ μs. Therefore a low-cost Q-switch fiber laser with ≈ 100 ns pulse would be capable of slicing the filament with minimum edge damage. Relatively low power system shown in Fig. 1a is capable of slicing filaments at 300 mm/s, which translates into production rate of 500 m/hr for a 10 filament cable.

Fig. 4a shows width the filament width as a function of the filament position recorded by an automated optical image recognition system. The filament width stayed within 50 μm over 10 m, length. The filament width variability is explained by the tape motion under the action of the assist gas. Fig. 4b-c present SEM images of 1 mm wide cable variants: flat stack (b), and twisted stack (c). The micrograph clearly shows the Nichrome wire wrap. The cables allow for twisting with 40 mm pitch before onset of the critical current degradation. At 77 K the-8

filament cable has critical current density of 160 ± 10 A over 3 meters and 4-filament one 80 ± 7 A over 2.5 meters.

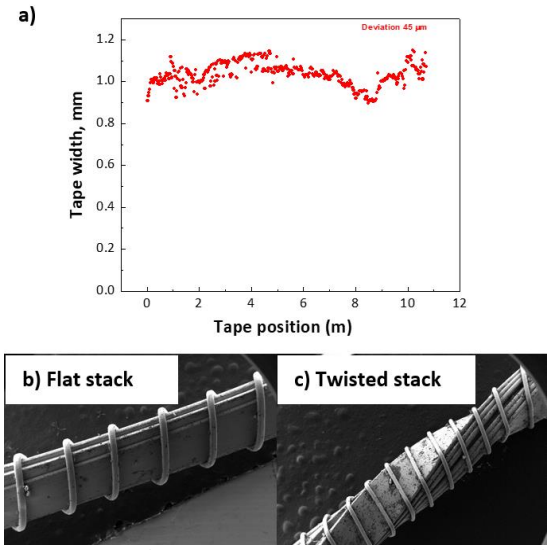

Fig. 4. (a) The 1 mm filament width vs. position profile, 10 meters filament length. (b) Scanning electron micrographs of 1.2 mm stack of exfoliated filaments. (c) Twisted stack.

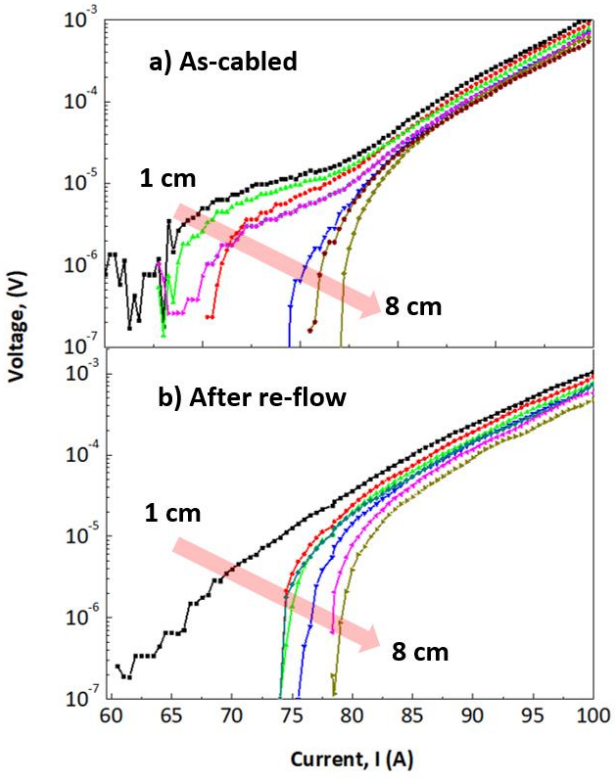

Fig. 5. Effect of solder re-flow on current sharing in a 4 filament 1 mm cable. (a) *I-V* curves recorded using voltage taps spaced at 1 cm increments from the current lead. (b) The same set of *I-V* curves after the re-flow step, 185ºC, 10 min.

Fig. 5 demonstrates effect of solder re-flow on the current transfer length in a four-filament cable coupon. Here *I-V* curves are recorded at 1 cm intervals from the current lead. The current redistribution is clearly seen as separation of I-V curves at < 10-5 V. As the current increases and the superconducting layer becomes more resistive the current re-distributes between the filaments. This is because the length of current transfer length

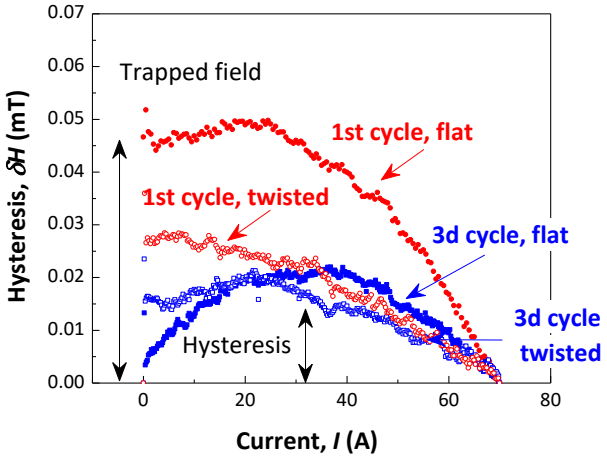

Fig. 6. Magnetic field hysteresis of a 8 turn coil wound from a flat cable and a cable subjected to 40 mm twist.

from normal metal to superconductor depends as $\sim R_d^{-1//2}$, where R_d is differential resistivity of the superconductor at given current [15, 16]. After the re-flow the inter-filament resistivity decreases from 1 m Ω×cm^2 to 200 – 500 μΩ×cm^2 and the current is fully transferred into the filament stack at a distance less than 1 cm, see Fig. 5b.

Finally, in Fig. 6 we compare hysteresis of a test coil manufactured from a flat cable and cable twisted with 40 mm pitch. The coils show a proportional reduction in the magnetic field hysteresis, however the twist has minor effect on the field hysteresis, in agreement with digital models that predict ≈ 50% reduction of magnetic moment due to the twist [17].

IV. Conclusion

A conclusion we demonstrate a feasibility of manufacturing 1 mm wide cables using exfoliated YBCO filaments. The major difficulty of the cabling process is handling narrow and delicate filaments. There is a need for a cabling method that would slice, bundle and cable filaments in single pass, preferably starting from a wide, 50 – 100 mm tape. The cabling method would thus eliminate or at least minimize a possibility of damaging the YBCO layer during re-spooling and priming.

Acknowledgment

The authors wish to thank Martin Rupich of American Superconductor Corporation for providing the 2G wire coupons, Chung-Chueh Chang of Stony Brook University for scanning electron microscopy and differential scanning calorimetry measurements.

REFERENCES

[1] K. L. Kim, J. B. Song, D. G. Yang, Y. G. Kim, T. H. Kim, S. K. Kim, *et al.*, "Study on elimination of screening-current-induced field in pancake-type non-insulated HTS coil," *Superconductor Science and Technology*, vol. 29, p. 035009, 2016.

[2] A. Naoyuki, O. Hiroaki, S. Takuya, N. Taketsune, O. Toru, K. Kei, *et al.*, "Temporal behaviour of multipole components of the magnetic field in a small dipole magnet wound with coated conductors," *Superconductor Science and Technology*, vol. 28, p. 035003, 2015.

[3] G. Francesco and K. Anna, "How filaments can reduce AC losses in HTS coated conductors: a review," *Superconductor Science and Technology*, vol. 29, p. 083002, 2016.

[4] A. C. Wulff, M. Solovyov, F. Gömöry, A. B. Abrahamsen, O. V. Mishin, A. Usoskin, *et al.*, "Two level undercut-profile substrate for filamentary YBa 2 Cu 3 O 7 coated conductors," *Superconductor Science and Technology*, vol. 28, p. 072001, 2015.

[5] M. Vojenčiak, A. Kario, B. Ringsdorf, R. Nast, D. C. v. d. Laan, J. Scheiter, *et al.*, "Magnetization ac loss reduction in HTS CORC ® cables made of striated coated conductors," *Superconductor Science and Technology*, vol. 28, p. 104006, 2015.

[6] A. R. Insinga, A. Sundaram, D. W. Hazelton, V. M. R. Zermeno, A. B. Abrahamsen, Y. A. Opata, *et al.*, "Two Level Undercut-Profile Substrate-Based Filamentary Coated Conductors Produced Using Metal Organic Chemical Vapor Deposition," *Ieee Transactions on Applied Superconductivity*, vol. 28, Jun 2018.

[7] O. Tsukamoto and M. Ciszek, "AC magnetization losses in striated YBCO-123/Hastelloy coated conductors," *Superconductor Science and Technology*, vol. 20, p. 974, 2007.

[8] K. Suzuki, J. Matsuda, M. Yoshizumi, T. Izumi, Y. Shiohara, M. Iwakuma, *et al.*, "Development of a laser scribing process of coated conductors for the reduction of AC losses," *Superconductor Science and Technology*, vol. 20, p. 822, 2007.

[9] M. Takayasu, L. Chiesa, N. C. Allen, and J. V. Minervini, "Present Status and Recent Developments of the Twisted Stacked-Tape Cable Conductor," *IEEE Transactions on Applied Superconductivity*, vol. 26, pp. 25-34, 2016.

[10] M. J. Wolf, N. Bagrets, W. H. Fietz, C. Lange, and K. Weiss, "Critical Current Densities of 482 A/mm^2 in HTS CrossConductors at 4.2 K and 12 T," *IEEE Transactions on Applied Superconductivity*, vol. 28, pp. 1-4, 2018.

[11] J. D. Weiss, T. Mulder, H. ten Kate, and D. van der Laan, "Introduction of CORC ® wires: highly flexible, round high-temperature superconducting wires for magnet and power transmission applications," *Superconductor Science and Technology*, vol. 30, p. 014002, 2017.

[12] W. Goldacker, F. Grilli, E. Pardo, A. Kario, S. Schlachter, and M. Vojenčiak, "Roebel cables from REBCO coated conductors: a one-century-old concept for the superconductivity of the future," *Superconductor Science and Technology*, vol. 27, p. 093001, 2014.

[13] V. Solovyov and P. Farrell, "Exfoliated YBCO filaments for second-generation superconducting cable," *Superconductor Science and Technology*, vol. 30, p. 014006, 2017.

[14] P. Schaaf, *Laser processing of materials : fundamentals, applications and developments*. Berlin ; London: Springer, 2010.

[15] J. H. Kim, C. H. Kim, V. Pothavajhala, and S. V. Pamidi, "Current Sharing and Redistribution in Superconducting DC Cable," *IEEE Transactions on Applied Superconductivity*, vol. 23, Jun 2013.

[16] G. Levin, P. Barnes, and J. Bulmer, "Current sharing between superconducting film and normal metal," *Superconductor Science and Technology*, vol. 20, p. 757, 2007.

[17] T. Makoto, C. Luisa, B. Leslie, and V. M. Joseph, "HTS twisted stacked-tape cable conductor," *Superconductor Science and Technology*, vol. 25, p. 014011, 2012.